Environment International 183 (2024) 108349

Contents lists available at ScienceDirect

Environment International

journal homepage: www.elsevier.com/locate/envint

Full length article

Establishment of plastic-associated microbial community from superworm gut microbiome

Yi-Nan Liu [a,b,1], Sakcham Bairoliya [a,b,1], Norazean Zaiden [a,b], Bin Cao [a,b,*]

[a] School of Civil and Environmental Engineering, Nanyang Technological University, Singapore
[b] Singapore Centre for Environmental Life Sciences Engineering, Nanyang Technological University, Singapore

ARTICLE INFO

Handling Editor: Thanh Nguyen

Keywords:
Plastic-microbe interaction
Biofilm
Plastic-munching worms
Gut microbiome

ABSTRACT

Gut microbial communities of plastic-munching worms provide novel insights for the development of plastic-processing biotechnologies. Considering the complexity of worm maintenance and the gut microbial communities, it is challenging to apply the worms directly in plastic processing. Harnessing the power of microbial communities derived from the worm gut microbiomes in vitro may enable a promising bioprocess for plastic degradation. Here, we established stable and reproducible plastic-associated biofilm communities derived from the gut microbiome of a superworm, *Zophobas atratus*, through a two-stage enrichment process: feeding with plastics (HDPE, PP, and PS) and in vitro incubation of gut microbiomes obtained from the plastic-fed worms. Plastic feeding exhibited marginal influence on bacterial diversity but substantially changed the relative abundance of different bacterial groups, and intriguingly, enriched potential plastic degraders. More prominent shifts of microbial communities were observed during the in vitro incubation of the gut microbiomes. Taxa containing plastic-degrading strains were further enriched, while other taxa represented by lactic acid bacteria were depleted. Additionally, the plastic characterization confirmed the degradation of the incubated plastics by the plastic-associated microbial communities. Community functional inference for both gene abundance and community phenotype suggested that the in vitro incubation enhanced plastic-degrading potential. Deterministic ecological effects, in particular, selection processes, were identified as the main driving force of the observed community shifts. Our findings provide novel insights into plastic-munching-worm-inspired bioprocessing of plastic wastes.

1. Introduction

Over the last 70 years, 8,300 million tonnes of plastic materials have been manufactured. However, apart from 2,500 tonnes still in use, only 6 % of the manufactured plastic was recycled (Roser 2022). Due to their resistance to degradation, these plastics accumulate continuously in the aquatic (Jambeck et al., 2015) and terrestrial environments (Nizzetto et al., 2016), posing substantial threats to the ecosystems (Amaral-Zettler et al., 2020; Galloway et al., 2017) and human health (Leslie et al., 2022; Schwabl et al., 2019). There is an imperative need for us to manage used plastics in a more sustainable manner and create a valuable circular economy for plastic products. To meet this need, various approaches involving biodegradation (Ellis et al., 2021), chemical recycling (Zhang et al., 2022a), and mechanical processing (Ragaert et al., 2017) have been developed. Among them, biodegradation has gained increasing attention because of its environmental friendliness and high cost-effectiveness (Wei et al., 2020). A wide range of microorganisms have been identified to be potential plastic degraders, most of which were isolated from various terrestrial and aquatic environments (Danso et al., 2018; Hajighasemi et al., 2018; Yoshida et al., 2016).

In the past decade, the larvae of lepidopteran and coleopteran insects, such as *Tenebrio molitor* (Brandon et al., 2018), *Spodoptera frugiperda* (Zhang et al., 2022c), *Galleria mellonella* (Sanluis-Verdes et al., 2022), and *Zophobas atratus* (Kim et al., 2020), were found to be capable of breaking down plastics. The gut microbiomes of these plastic-munching worms serve as a new microbial source for plastic biodegradation (Pivato et al., 2022). For example, the screening of worm gut microbiomes has discovered new plastic-degrading bacterial strains such as *Klebsiella* sp. EMBL-1 (Zhang et al., 2022c), *Massilia* sp. FS1903

* Corresponding author at: School of Civil and Environmental Engineering, Nanyang Technological University, 50 Nanyang Ave, N1-01C-69, Singapore 639798, Singapore.
E-mail address: bincao@ntu.edu.sg (B. Cao).
[1] These authors contributed equally to this work.

https://doi.org/10.1016/j.envint.2023.108349
Received 5 September 2023; Received in revised form 21 November 2023; Accepted 22 November 2023
Available online 23 November 2023

Abbreviations

HDPE	High-density polyethylene
PP	Polypropylene
PS	Polystyrene
FTIR	Fourier-transform infrared spectroscopy
ASV	Amplicon sequence variant
NTI	Nearest taxon index
KO	KEGG Orthologies
NMDS	Nonmetric dimensional scaling
HeS	Heterogeneous selection
HoS	Homogeneous selection
DR	Drift

(Jiang et al., 2021), *Pseudomonas* sp. EDB1, *Bacillus* sp. EDA4, and *Brevibacterium* sp. EDX (Arunrattiyakorn et al., 2022). Despite the promising prospect, investigation into plastic-munching worms gut microbiomes is in its infancy. Although different feeding strategies have been reported to shape the gut microbial community structures and influence the microbiome functions in worms (Brandon et al., 2018; Luo et al., 2021; Peng et al., 2019), there has been no effective strategy to control or engineer the gut microbiome in vitro for improved plastic-degradation capability because of the limited understanding of the gut microbial community succession in in vitro conditions. In addition, considering the complexity of worm maintenance and the gut microbial communities, it is challenging to apply the worms directly in plastic processing (Billen et al., 2020). Harnessing the power of microbial communities derived from the worm gut microbiomes in vitro may enable a promising bioprocess for plastic degradation.

In this study, we aim to establish a stable and reproducible plastic-associated biofilm community derived from the gut microbiome of a superworm, *Zophobas atratus*. To achieve this, we applied a two-stage enrichment process: (i) plastic-feeding to condition the gut microbiome of the worms and (ii) in vitro incubation of the gut microbiomes with plastics. We examined the shifts of gut microbial communities in response to plastic feeding and monitored the microbial community succession during the in vitro incubation. We further identified the deterministic ecological effects as the main driving force of the community succession. Our study demonstrates the establishment of plastic-associated biofilm communities from the worm gut microbiome, which will facilitate the development of plastic-munching-worm-inspired bioprocessing for plastic waste upcycling.

2. Methods

2.1. Maintenance of superworms and plastic feeding

Five-week-old superworms (*Zophobas atratus*) with an average weight of ca. 0.7 g each were obtained from a local pet store. The worms were fed with oatmeal for 30 days before being transferred randomly into glass containers (40 worms each) and fed with 3 types of plastics (HDPE, PP, and PS) with 3 biological replicates for each type of plastic. The oatmeal-fed control group superworms continued to be fed with oatmeal for one month. The plastic materials utilized in this study are high-density polyethylene (HDPE) films (2.5 cm × 7.0 cm × 0.02 mm), polypropylene (PP) strips (5 cm × 1 cm × 0.25 mm), and polystyrene (PS) Styrofoam bars (1 cm × 1 cm × 5 cm). The frass was removed from the containers every three days. Because of the stronger resistance of HDPE and PP to worm chewing, the feedings of HDPE and PP lasted for one month, while the feeding of PS lasted for two weeks (Fig. 1).

2.2. Extraction of superworm gut microbiomes

After plastic feeding, the worms were dissected to extract the gut microbiomes. The worms were immersed in 75 % ethanol solution and rinsed twice with deionized water before being dissected. The guts were drawn out and vigorously vortexed in 0.9 % NaCl solution, filtered through a 10-μm filter (pluriStrainer Mini 10 μm, PluriSelect) to remove worm tissue, and centrifuged at 10000 rpm for 10 min to harvest gut microbial communities.

2.3. In vitro incubation of superworm gut microbial communities

For each plastic-fed superworm group (HDPE, PP, and PS), gut bacteria harvested from 30 superworms were inoculated into 30 mL of Bushnell–Haas medium (Wright et al., 2020) with respective plastics. Given the different densities of plastics, the amounts of added plastics were 0.12 g for PS flakes (1.0 cm × 1.0 cm × 0.2 cm) and 0.20 g each for HDPE (2.5 cm × 7.0 cm × 0.02 mm) films and PP (5.0 cm × 1.0 cm × 0.25 mm) strips. Before incubation, the plastics were sterilized with 75 % ethanol and dried in a biological safety cabinet. Gut bacteria of the oatmeal-fed control group were also harvested and inoculated into 30 mL of Bushnell–Haas medium without plastics. The in vitro incubation experiment was conducted in four replicates and lasted for six weeks at 25 ℃ in the dark (Fig. 1). Two mL of bacterial suspension and one piece of plastic were collected weekly, and 2 mL of fresh Bushnell-Haas medium was added to the Erlenmeyer flask to maintain the total volume of

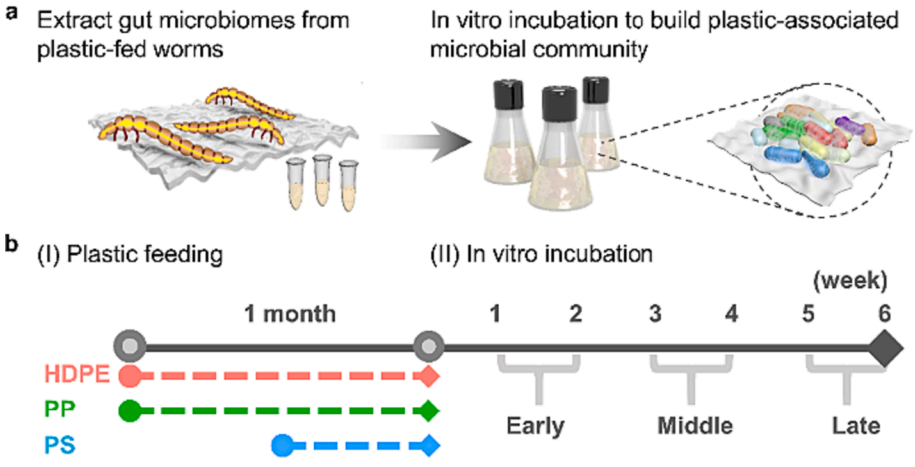

Fig. 1. Schematic illustration of experimental design for the establishment of plastic-associated microbial communities from superworm gut microbiomes. (a) First, superworms were fed with plastics (HDPE, PP, and PS) for half to one month. Then, their gut microbiomes were extracted and further incubated in the flasks containing culture media and respective plastics. (b) Timeline of the two-stage microbiome enrichment.

30 mL. All the samples were stored at −20 °C before DNA extraction.

2.4. Characterization of plastic samples

Physicochemical properties of the original plastics and the plastic samples taken at the late stage of incubation were characterized. Before surface characterization, the plastic samples were immersed in 2 % sodium dodecyl sulfate solution for 4 h. Then, the soaked plastics were washed with deionized water and dried at 60 ℃ overnight. The Fourier-transform infrared (FTIR) spectra of plastic samples were acquired on an FTIR spectrometer (Frontier, Perkin Elmer Instrument, Waltham, USA) in the attenuated total reflectance mode. The spectral resolution was set as 1 cm^{-1}, and the scanning range was from 600 to 4000 cm^{-1}. The scanning of both the original and incubated plastics (with or without microbial inoculum) were repeated 16 times to improve the signal-to-noise ratio. The water contact angles of the plastic surfaces were quantified by a video contact angle system (VCA-optima, AST Inc., USA). For each sample, the measurement was repeated at least 6 times. Thermal stability analysis of plastic samples was conducted by using a thermogravimetric analyzer (TGA4000, Perkin Elmer, Netherlands), during which original and incubated plastic sample was heated from ambient temperature to 800 ℃ with a rate of 20 ℃/min in nitrogen atmosphere.

2.5. DNA extraction and 16S rRNA gene amplicon sequencing

The DNA from the plastic (biofilm) and bacterial suspension (planktonic bacteria) samples was extracted using the DNeasy Powersoil Kit (Qiagen, Germany) and cleaned up using the Genomic DNA Clean & Concentrator (ZymoResearch, USA) following the manufacturers' protocols. The V4 and V5 regions of 16S rRNA genes were amplified using the primers 515F (5′-GTGCCAGCMGCCGCGG-3′) and 907R (5′-CCGTCAATCMTTTRAGTTT-3′) (Yang et al., 2020). PCR was carried out in a 25-μL reaction volume containing 2 μL DNA template (10 ng/μL), 0.5 μL forward primer solution (10 μM), 0.5 μL reverse primer solution (10 μM), 9.5 μL nuclease-free water (New England, USA), and 12.5 μL KAPA ReadyMix (HiFi HotStart, Roche, Switzerland). The amplicons were purified using the AMPure XP beads (Beckman Coulter, USA) and quantified using the Qubit dsDNA HS assay kit (Thermo Fisher Scientific, USA). Following library preparation and quality control, pair-end sequencing (300 bp × 300 bp) was carried out on an Illumina MiSeq platform.

2.6. Processing of sequencing data

Amplicon sequences were processed using the DADA2 pipeline (version 1.8) and aligned to the SILVA 132 database in R (version 4.1.1) (Callahan et al., 2016). The obtained amplicon sequence variant (ASV) tables were utilized to analyse the shift in microbial communities. The ASV tables were resampled to the same library size with the R package Vegan (Oksanen et al., 2022). The α- and β-diversities of the microbial communities were calculated with the R package phyloseq (McMurdie and Holmes 2013). Nearest taxon index (NTI) and β-NTI were calculated by using the R package picante (Kembel et al., 2010). The relative importance of different ecological processes in the community assembly was quantified by using the R package iCAMP(Ning et al., 2020). The differential abundance between microbial groups was analysed by using the STAMP software (White's non-parametric *t*-test with BH correction) (Parks et al., 2014). The statistical analyses of community dissimilarities were performed using permutational multivariate analysis of variance (PERMANOVA; R packages vegan and pairwise Adonis). The statistical analyses of Shannon indices, NTI, and null model results were conducted by the Kruskal–Wallis test and the pairwise Wilcoxon test (with BH correction). The 68 % confidence ellipses were presented on the two-dimensional non-metric multidimensional scaling plots to illustrate the one standard deviation regions of the mean values.

Potential functions of the microbial communities were predicted by using PICRUSt2 and FAPROTAX (Douglas et al., 2020; Louca et al., 2016). Abundances of KEGG Orthologies (KO) and MetaCyc pathways were predicted based on the amplicon sequencing data by PICRUSt2. Ecologically relevant phenotypes were inferred based on the default database and a plastic-degrading microorganism database (PlasticDB) (Gambarini et al., 2022) by FAPROTAX.

The raw sequencing data have been deposited in the NCBI SRA database (BioProject ID: PRJNA948638). The R scripts used in the processing of the sequencing data are available in the GitHub repository (https://github.com/liuyinan19922/Worm-gut-microbiome).

3. Results

3.1. Plastic-specific shift in the gut microbiome in response to plastic feeding

With the ultimate goal of enriching potential plastic-degrading microbiomes, we fed the superworms with different plastics (HDPE, PP, and PS) for half to one month (Fig. 1). The amount of consumed plastics increased with time, causing apparent damage on the edges of the plastics (Fig. S1). After plastic feeding, the α-diversity metrics of gut communities remained stable with no significant change compared to that of the plastic-free group ($P > 0.05$, Kruskal–Wallis test; Fig. S2). All the gut microbiomes had a Shannon index around 4 (Fig. 2a), suggesting a comparable taxonomic diversity. Consistent with this observation, the NTIs of plastic-fed microbiomes were also close to that of plastic-free group microbiome ($P > 0.05$, Kruskal–Wallis test; Fig. 2b), suggesting a limited influence of the plastic feeding on the diversity of worm gut communities. In addition, all these gut microbiomes had an NTI larger than 2 (away from the 2-fold standard deviations of null expectation, $P < 0.05$), implying that the gut microbiomes were phylogenetically more clustered than a random community. Based on the Bray–Curtis dissimilarity, the nonmetric dimensional scaling (NMDS) analyses show a significant difference in the microbial community structures among the plastic-fed and plastic-free groups ($P = 0.001$, PERMANOVA test), where different feeding groups form distinct clusters (Fig. 2c). However, the 68 % confidence ellipses (one standard deviation confidence regions of mean values) of HDPE, PP, and plastic-free groups overlapped. Corresponding pairwise PERMANOVA tests show no significant difference among them ($P > 0.05$) and a slight shift of microbiomes after feeding with PP and HDPE. The plastic-fed and plastic-free microbiomes contained similar dominant genera and shared 8 out of the 10 most abundant genera (Table S1 and Fig. 2d): *Chryseobacterium* (32.93–55.58 %), *Enterococcus* (9.03–17.38 %), *Dysgonomonas* (12.91–8.33 %), *Lactococcus* (1.91–21.02 %), *Pseudomonas* (4.78–10.30 %), *Morganella* (4.33–5.47 %), *Lactobacillus* (0.82–1.55 %), and *Enterobacter* (0.74–1.53 %).

However, the relative abundances of the dominant genera varied substantially with certain genera being enriched or depleted in the plastic-fed groups compared with the plastic-free gut microbiome (Fig. 2e–g and Table S2). The enriched ones were plastic-type-specific. For example, *Pseudomonas* was enriched in the gut microbiomes of worms fed with HDPE and PP, while *Morganella* and *Enterobacter* were enriched in the gut microbiomes of PP- and PS-fed worms. Moreover, in the gut microbiomes of the plastic-fed worms, many of the enriched genera, such as *Pseudomonas*, *Enterobacter*, *Chryseobacterium*, and *Citrobacter*, are known to contain plastic-degrading bacterial strains (Table S3 and Fig. 2e–g). This result suggests the selection effect of plastic diets on worm gut microbiomes. The enrichment of some genera has also been reported in previous studies: *Citrobacter* and *Enterobacter* were found to be enriched in the gut microbiome of PP-fed superworms (Yang et al., 2021), and *Pseudomonas* was found to be enriched in the gut microbiome of PS-fed greater wax moth larvae (Lou et al., 2020). In contrast, the depleted genera were similar in the three plastic-feeding groups. For example, *Lactococcus* was depleted in all the plastic-

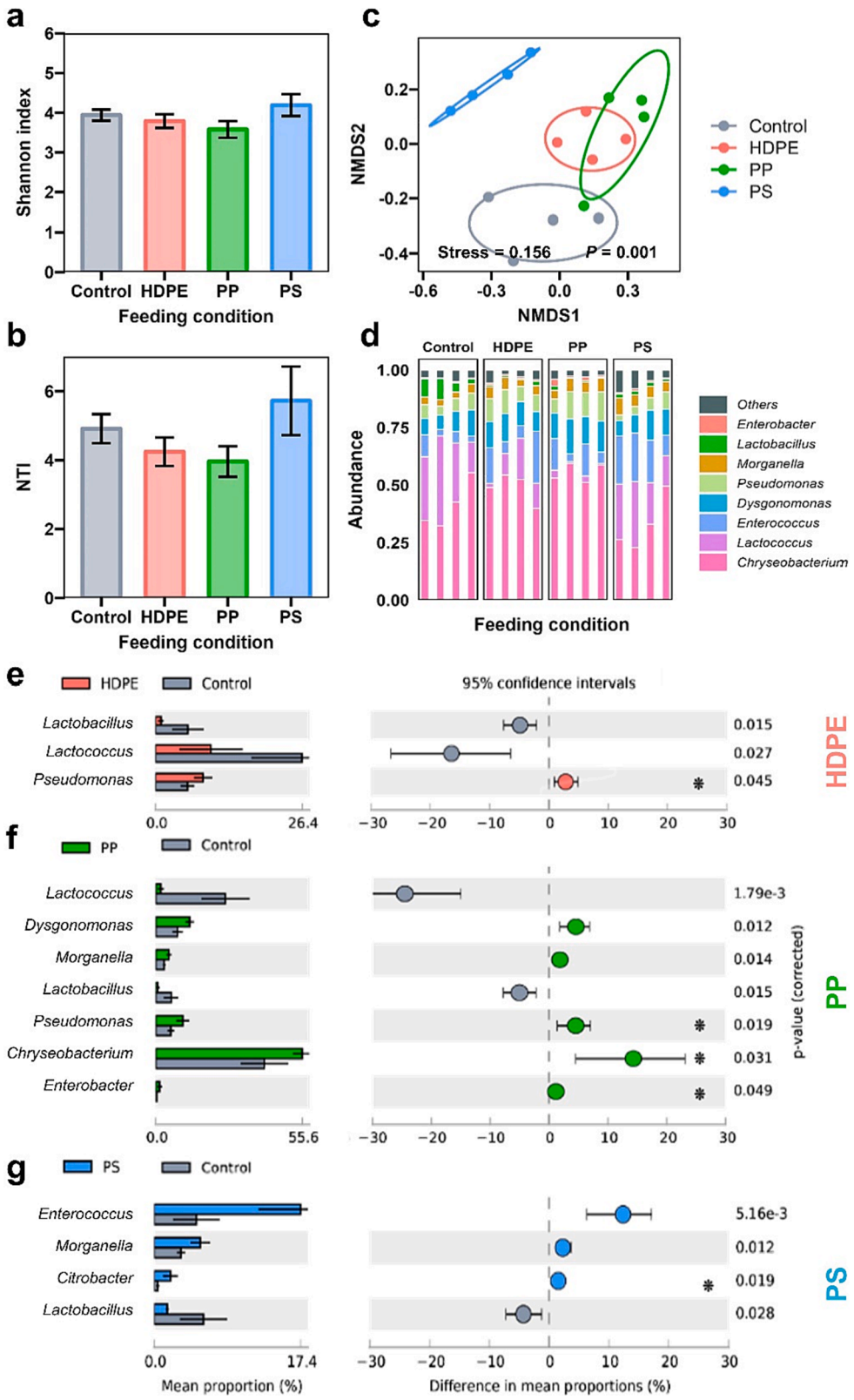

Fig. 2. Plastic-specific shift in the gut microbiome in response to plastic feeding: (a) The Shannon indices and (b) NTIs of gut microbial communities from plastic-fed worms. The error bars represent the standard deviations. (c) NMDS ordinations of gut microbial communities based on the Bray–Curtis dissimilarity. The ellipses indicate the 68 % confidence regions. (d) Gut microbiome compositions after plastic feeding at the genus level. The four columns in each box represent the results of four biological replicates under each feeding condition. (e–g) Differential abundance analysis of plastic-fed gut microbiomes (e: HDPE group; f: PP group; g: PS group) compared to that of the oatmeal-fed control group at the genus level (proportion change > 1 % and $P < 0.05$ (White's non-parametric *t*-test)). * in the figures indicates the genus that contains reported plastic-degrading strains.

feeding groups, and *Lactobacillus* was depleted in the HDPE and PP groups. Both *Lactococcus* and *Lactobacillus* are lactic acid bacteria contributing considerably to carbohydrate fermentations (Hatti-Kaul et al., 2018; Pessione, 2012). Their depletion could be attributed to the diet change from carbohydrate-rich oatmeal to plastics. Collectively, our results show that plastic-feeding exhibited marginal influence on bacterial diversity but substantially changed the relative abundance of different bacterial groups, and intriguingly, enriched potential plastic degraders in the gut microbiomes.

3.2. Microbial community succession during in vitro incubation of gut microbiomes

Following plastic feeding, we extracted the gut microbiomes from the plastic-fed worms and inoculated them into flasks with a carbon-free medium and plastics (Fig. 1). We hypothesize that the in vitro

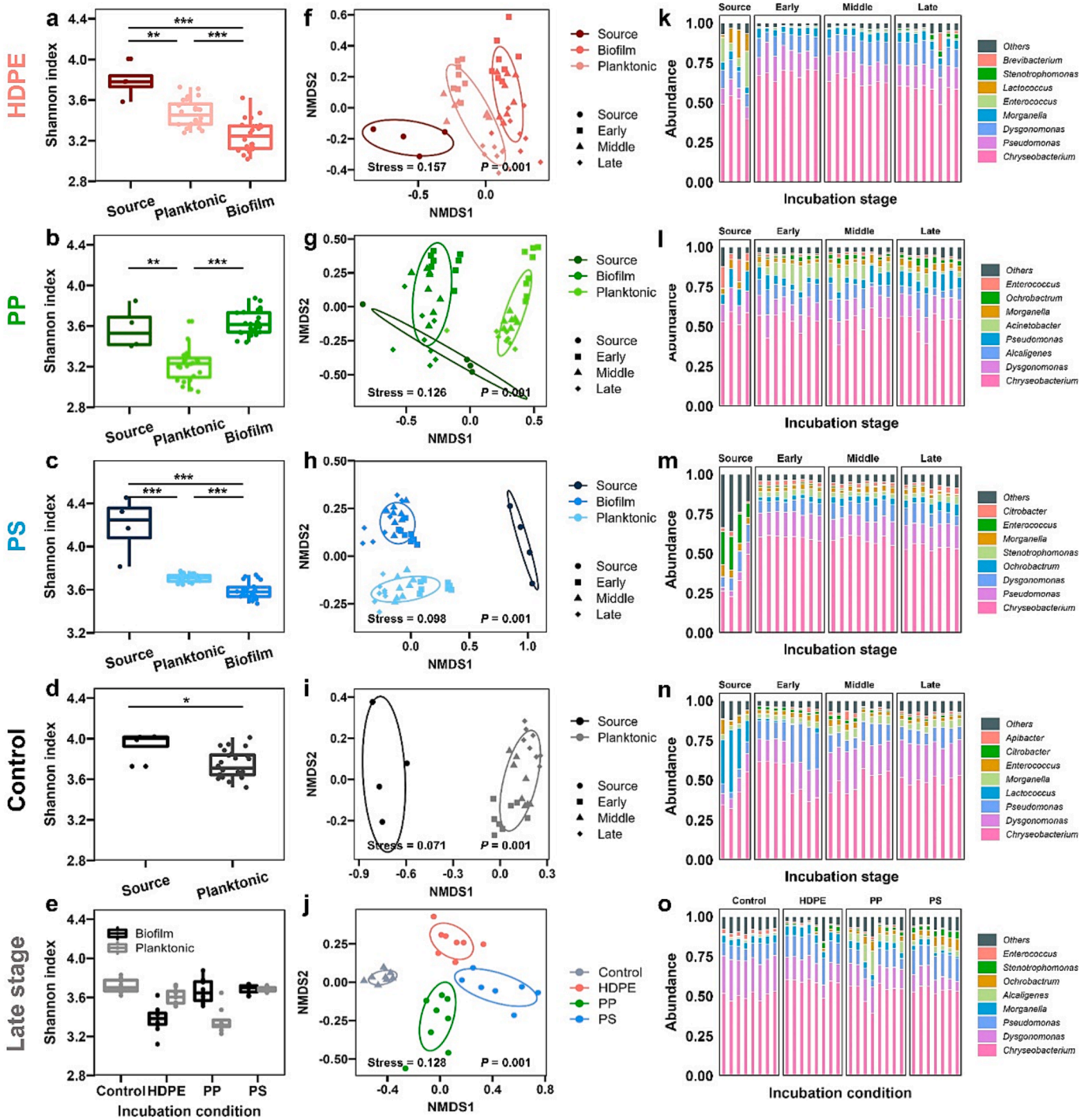

Fig. 3. Shifts of the microbial communities during in vitro incubation. The Shannon indices (a: HDPE group; b: PP group; c: PS group; d: plastic-free control group; e: comparison among different groups at the late stage) and the NMDS ordinations (f: HDPE group; g: PP group; h: PS group; i: plastic-free control groups; j: comparison among different biofilm communities at the late stage) of the incubated microbial communities. The changes in biofilm microbial community compositions during the incubations (k: HDPE group; l: PP group; m: PS group; n: plastic-free control group; o: comparison of different groups at the late stage). *, **, and *** indicate $P < 0.05$, $P < 0.005$, and $P < 0.001$, respectively.

incubation facilitates the enrichment of potential plastic-degrading strains, resulting in a reduced complexity of the microbiome. Consistent with our hypothesis, the in vitro incubation resulted in a significant change in the taxonomic richness and evenness of microbial communities (Fig. 3a–c and S2). The obtained planktonic and biofilm communities, except for PP-associated biofilms, displayed significantly lower Shannon indices than those of the inoculation sources (i.e., the obtained plastic-fed gut microbiomes in the first-stage enrichment). For HDPE and PS groups, the Shannon indices of the plastic-associated biofilm communities exhibited even lower than those of corresponding planktonic communities ($P < 0.05$, Kruskal–Wallis test). At the late stage (the 5th and 6th weeks), the incubated communities showed a Shannon index ranging from 3.38 to 3.72 (Fig. 3e), which is lower than that of the plastic-free worm gut microbiome (3.94 ± 0.14).

The NMDS analysis shows that the plastic-associated biofilms and the planktonic communities formed distinct clusters ($P = 0.001$, PERMANOVA test; Fig. 3f–i). The microbial communities of different plastic-incubation groups at the late stage also separated from each other ($P < 0.05$, pairwise PERMANOVA test with BH correction, Fig. 3j and S4), suggesting that the addition of different plastics diverged the successions of the microbial communities. For each plastic-incubated group, the microbial community composition changed substantially at the early stage and stabilized at the late stage (Fig. 3k–o and S5, Tables S4 and S5). Compared with the inocula, although *Chryseobacterium* was still the most abundant genus (51.11–58.16 %), the other dominant genera in the inocula were replaced at the late stage of incubation. There are only 4 common genera among plastic-incubated and plastic-free groups in the ten most abundant genera: *Chryseobacterium* (51.11–58.16 %), *Dysgonomonas* (8.46–14.38 %), *Pseudomonas* (8.71–14.29 %), and *Morganella* (2.23–5.66 %). Meanwhile, *Stenotrophomonas* (1.38–5.89 %) and *Ochrobactrum* (0.82–7.61 %) emerged as the dominant genera in the plastic-incubated microbiomes.

To further evaluate the community structure changes, we analysed the differentially abundant genera in the incubated microbiomes (Fig. 4a–c and S6, Table S6 and S7). Compared with plastic feeding, more genera were enriched or depleted after the in vitro incubation in both the biofilm and planktonic communities. The enriched genera in different plastic incubated groups contained common members. For example, *Stenotrophomonas* and *Ochrobactrum* were enriched in all biofilm communities, while *Stenotrophomonas* and *Alcaligenes* were enriched in all planktonic communities. Meanwhile, different plastic groups also have their specific enriched taxa. *Pseudomonas*, *Chryseobacterium*, *Acinetobacter, Morganella*, *Dysgonomonas*, and *Methylobacterium* were only enriched in one or two plastic incubation groups.

Notably, regardless of biofilm or planktonic communities, nearly all the enriched genera contain previously reported plastic-degrading strains (Table S3, Fig. 4a–c and S6). In contrast, in the plastic-free group, only one third of the enriched genera contain plastic-degrading strains (3 out of the 9 enriched genera), and their abundance increments were limited (0.79 %, 1.07 %, and 3.36 % for *Citrobacter*, *Alcaligenes*, and *Pseudomonas*, respectively; Fig. 4d and Table S7). The depleted genera were similar among the plastic-incubated communities: *Enterococcus* and *Lactococcus* were depleted in all incubated communities, and *Lactobacillus* was depleted in the biofilm communities of HDPE and PP groups. All these depleted genera are lactic acid bacteria. From the gut environment to a carbon-free medium, the concentrations

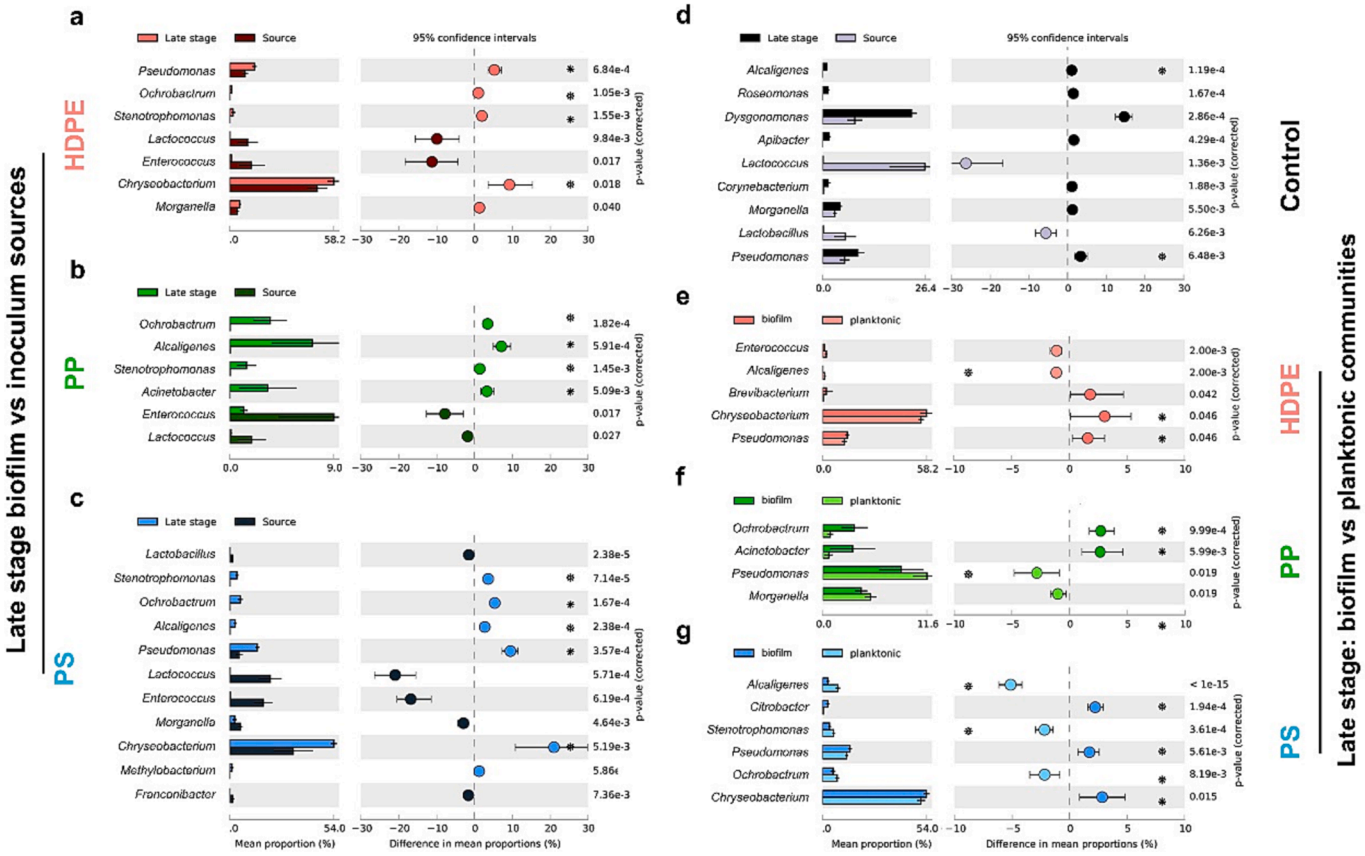

Fig. 4. Differential abundance analysis of microbial communities after in vitro plastic incubation. (a–d) Enriched and depleted genera in biofilm communities compared to their inoculum sources (a: HDPE group; b: PP group; c: PS group; d: plastic-free control groups; proportion change > 1 % and $P < 0.05$ (White's non-parametric *t*-test)). (e–g) Enriched and depleted genera in biofilm communities compared with their corresponding planktonic communities (e: HDPE group; f: PP group; g: PS group; proportion change > 1 % and $P < 0.05$ (White's non-parametric *t*-test)). * in the figures indicates the genus that contains reported plastic-degrading strains.

of organic nutrients decreased severely, which may have further inhibited fermentative bacteria.

In addition, we also compared the differentially abundant genera between the biofilm and planktonic communities in each group (Fig. 4e–g and Table S8). Although the dominant genera of biofilm and planktonic communities within a specific group are similar, their relative abundance differs. The distribution of taxa between biofilm and planktonic communities can be attributed to the different ecological niches of plastic surfaces and suspension. Some genera can be selectively enriched in biofilms by their plastic-degrading or adhesion ability. Moreover, the differentially abundant taxa varied with plastic types, and both the enriched and depleted genera contained reported plastic-degrading strains. For instance, *Ochrobactrum* was enriched in PP-associated biofilms but depleted in the HDPE- and PS-associated biofilms. In contrast, *Pseudomonas* was depleted in the PP-associated biofilms but enriched in the HDPE- and PS-associated biofilms. In addition, both the planktonic and biofilm communities enriched genera that contain reported plastic-degrading strains (marked with * in Fig. 4e–g). These results imply that biofilm–suspension distributions of taxa did not solely depend on whether the given taxon is a plastic degrader, and can also be associated with the physiochemical properties of plastics or substrate preferences of degrading strains.

3.3. Plastic surface characterisation and potential microbial functions

To gain functional insight into the plastic-associated microbiomes, we characterized the interfacial properties of plastics and predicted the potential functions of the enriched communities. We used FTIR spectra to infer the changes of different functional groups. To ensure the inference is reliable, we rinsed the samples to avoid the interference of biomass with FTIR spectra, followed the general interpretation process for infrared spectra, and referred to the peak assignments reported in

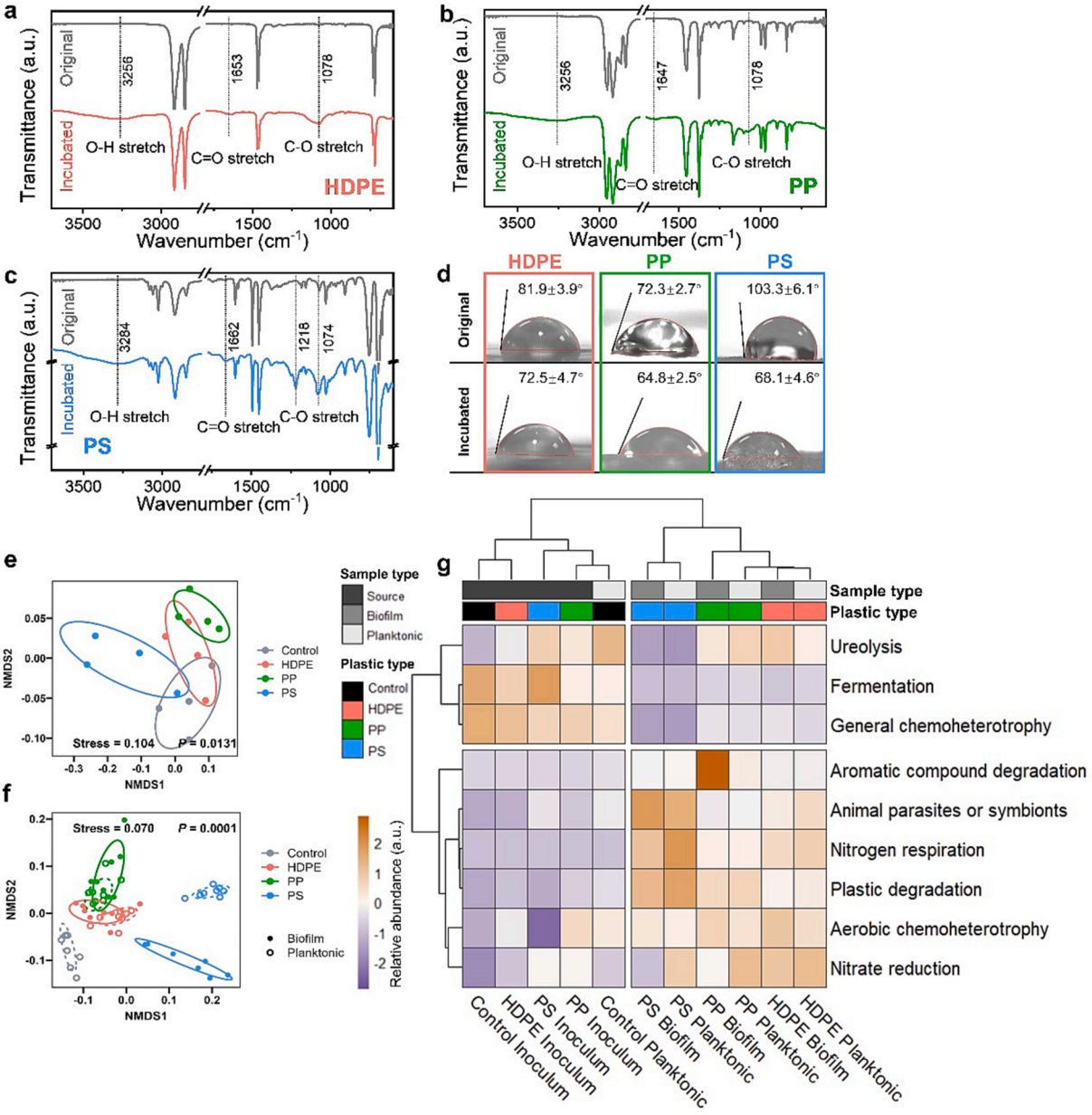

Fig. 5. Surface characterization of plastics and functional inference of microbiomes. (a–c) FTIR spectra of plastics before and after the incubation (a: HDPE sample; b: PP sample; c: PS sample). (d) The decrease in water contact angle after the in vitro incubation. The water contact angles were marked in d (n = 6). (e–f) NMDS ordinations of inferred KEGG Orthology abundances in microbial communities (e for the comparison of different microbial inocula and f for the comparison of different groups at the late stage). (g) Clustered heatmap of inferred community phenotypes of microbial inocula and late-stage communities.

recent studies on plastic biodegradation. In addition, we included plastics in Bushnell–Haas medium without microbial inoculum as an abiotic control, allowing us to confidently assign emerging peaks attributed to microbial processes (Fig. S7). After a 6-week in vitro gut microbiome incubation, we observed several new peaks in the FTIR spectra of all the three types of plastics, but not in the abiotic incubated samples without inoculum addition (Fig. 5a–c and S7). The emerging peaks exhibited similar wavenumbers: ~3250, ~1650, and ~ 1070 cm^{-1}, corresponding to O–H, C = O, and C–O stretching vibrations, respectively (Brandon et al., 2018; Coates, 2006; Kim et al., 2020; Yang et al., 2014). We also compared the hydrophobicity of these plastic samples. For all the three types of plastics, the water contact angles decreased significantly after the incubation ($P < 0.05$, Kruskal–Wallis test; Fig. 5d). The reduced hydrophobicity suggests an elevated content of hydrophilic functional groups on the plastic surfaces, which is consistent with the results of FTIR spectra. Additionally, we quantified the thermal stability of the plastic samples before and after the in vitro incubation. All the weight loss curves of plastic samples exhibited only one pyrolysis. After in vitro incubation, the weight loss curves shifted to a lower temperature (Fig. S8a–c). Correspondingly, the first derivative curves of the weight loss curves showed one pyrolysis peak and the incubated plastic samples exhibited a lower pyrolysis peak temperature than those of the original plastics (Fig. S8d–f). The left-shifted weight loss curves and the lower pyrolysis peak temperature suggested a reduced thermal stability of the incubated plastics, which can be attributed to the depolymerization of plastic during in vitro incubation. Taken together, the presence of newly formed oxygen-containing functional groups, the increased surface hydrophilicity, and reduced thermal stability confirmed the plastic-degrading capability of the plastic-associated microbial communities.

To investigate the functional evolution of the microbiomes during the two-stage enrichment, we inferred their community functional profiles based on the amplicon sequencing data. We analyzed the β-diversity of PICRUST2-predicted KO and found that the change in community KO compositions share a similar trend with that of taxonomic compositions. During the first-stage enrichment (plastic-feeding), only a slight shift in functional profiles was observed. Although the overall statistical test reveals different distributions among community KO compositions ($P = 0.0131$, PERMANOVA test), the subsequent pairwise comparison indicates no significant difference between specific plastic-fed gut microbiome and the oatmeal-fed control group ($P < 0.05$, pairwise PERMANOVA test with BH correction, Fig. 5e). However, during the second-stage enrichment (in vitro incubation), the shift was found to be more prominent ($P = 0.0001$, PERMANOVA test; Fig. 5f and S9). All the microbiomes at the late stage of the incubation exhibited a significantly different functional profile compared with that of the plastic-free control group ($P < 0.05$, pairwise PERMANOVA test with BH correction).

The accuracy of amplicon-based functional prediction depends on the quality of sequencing data, the completeness of reference databases, and the complexity of microbial communities (Djemiel et al., 2022). To improve the quality of our sequencing data, we used the DADA2 pipeline to de-noise the raw data and infer exact amplicon sequence variants. The obtained worm gut microbiomes were well annotated, with 94.23 % of reads annotated to the genus level. For a wide coverage reference database, we utilized PICRUSt2 for functional gene prediction because of its larger database (IMG database) (Douglas et al., 2020). Additionally, we supplemented the FAPROTAX reference database with a plastic-degrading microorganism database (PlasticDB) for the community phenotype prediction. In addition, our analysis revealed that the superworm gut and incubated microbiomes exhibited a comparatively simple structure with less than 10 genera with an abundance of over 1 % (Tables S1, S4, and S5), which facilitated the community functional predictions.

FAPROTAX-predicted functions revealed distinct phenotypes between the incubated communities (biofilm and planktonic communities) and the inoculum source samples (Fig. 5g). The samples before and after the in vitro incubation could be divided by hierarchical clustering. After the in vitro incubation, the potentials for plastic degradation, aromatic compound degradation, and nitrogen respiration were significantly enhanced, while those for fermentation and general chemoheterotroph were weakened ($P < 0.05$, Kruskal–Wallis test).

The inference of pathway abundances also yielded similar results (Tables S9 and S10). Eight of the 16 commonly enriched pathways were predicted to be degradation pathways. In contrast, the majority of the commonly depleted pathways (12 out of 19) were involved in biosynthesis, fermentation, and assimilation. The biodegradation of HDPE, PP, and PS involves initial hydroxylation of the C-C backbone bonds, oxidation to corresponding ketones and alkanoic acids, and the final β-oxidation (Yeom et al., 2022; Zhang et al., 2022b). Several enzymes observed in the enriched degradation pathways could contribute to these processes. For instance, monooxygenases (in PWY-5651, PWY-7431, and PWY-5181) and hydroxylases (in PWY-5181) may participate in the initial hydroxylation of the plastics. Alcohol dehydrogenases (in PWY-5181) and aldehyde dehydrogenases (in PWY-5181 and PWY-7431) may catalyze the subsequent oxidation to ketones and alkanoic acids, respectively. In addition, dioxygenases (in PWY-5651, PWY-5181, and PROTOCATECHUATE-ORTHO-CLEAVAGE-PWY) may play an important role in the cleavage of benzene rings in PS (Zhang et al., 2022b). Both the predictions of phenotypes and pathway abundances suggest that the in vitro incubation enhanced plastic-degrading potential and weakened fermentation capacity.

3.4. Driving forces of the community shifts

The obtained NTIs of the microbial communities shared a similar trend to the taxonomic α-diversity metric: all the plastic-incubated groups (except the biofilm community in the PP group) had a lower NTI than their inoculum sources ($P < 0.05$, Kruskal–Wallis test; Fig. 6a–c). In contrast, for the plastic-free group, there is no significant difference between the NTI of the inoculum source and incubated communities (Fig. S10). These results suggest that the plastic incubation mitigated the phylogenetic clustering in the incubated communities. Moreover, all the obtained NTIs are larger than 2 (away from the 2-fold standard deviation of null expectation, $P < 0.05$), indicating that the incubated communities were not formed randomly. We also calculated β-NTIs between the incubated communities and their inoculum sources. A higher β-NTI corresponds to a greater phylogenetic β-diversity between two communities (compared to the null expectation), which is associated with a more important contribution of deterministic processes in the community assembly. The β-NTIs are shown in Fig. 6d–f (biofilm communities) and S11 (planktonic communities). In the early incubation stage, HDPE, PS, and plastic-free groups had β-NTI median values less than 2 (within the 2-fold standard deviation of null expectation, $P > 0.05$). At the middle and late stages of the incubation, all groups had β-NTIs larger than 2 ($P < 0.05$). These results imply the increased importance of deterministic processes in the assemblies of plastic-incubated communities during the incubation.

We further applied the iCAMP framework to quantify the relative contributions of different ecological processes in the assembly of plastic-incubated communities (Fig. 6g–i for biofilm communities and Fig. S12 for planktonic communities) (Ning et al., 2020). Three processes were found to drive the assemblies of incubated communities in the late stage: homogeneous selection (relative importance: 58.9–83.4 %), drift (11.1–33.4 %), and heterogeneous selection (0.7–21.6 %). The dominant contribution of selection processes validated plastics as ecological niches for microbes. Homogeneous selection results in lower turnover within phylogenetic bins. Thus, the greatest importance of homogeneous selection is consistent with the results of microbial community shifts that plastic-degrading genera were enriched and fermentative bacteria were depleted. We also compared the relative importance of ecological processes in the early and late incubation stages. The

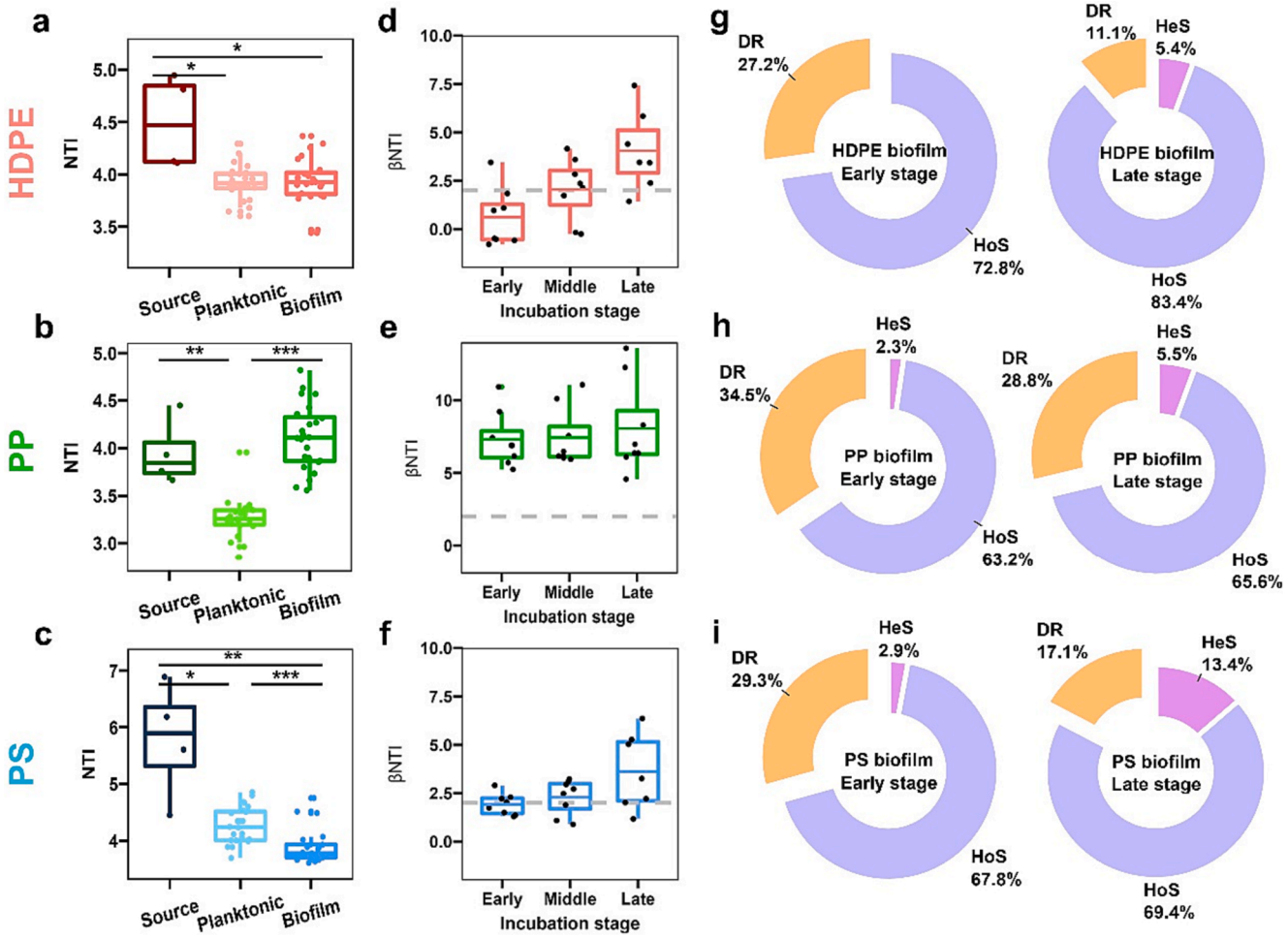

Fig. 6. Contributions of deterministic and stochastic processes in the microbial community assemblies during in vitro incubation. (a–c) The NTIs for different plastic incubation groups (a: HDPE group; b: PP group; c: PS group). (d–f) The β-NTIs of the biofilm communities of different plastic incubation groups (d: HDPE group; e: PP group; f: PS group). (g–i) The relative importance of different ecological processes (i.e. heterogeneous selection (HeS), homogeneous selection (HoS), and Drift (DR)) in the assemblies of the biofilm microbial communities (g: HDPE group; h: PP group; i: PS group). *, **, and *** indicate $P < 0.05$, $P < 0.005$, and $P < 0.001$, respectively.

importance of total selection (including both heterogeneous and heterogeneous selections) in the late stage was significantly higher than that in the early stage ($P < 0.05$, Kruskal–Wallis test), which is in line with the β-NTI results, suggesting an increased contribution of selection with prolonged incubation duration. In addition, heterogeneous selection also became more important at the late stage, which could be attributed to the emergence of heterogenous microenvironments in mature biofilms.

4. Discussion

Previous analyses of plastic-munching worm gut microbiomes mainly aimed to confirm microbial contribution to plastic degradation and reveal the influence of diets on the microbiome composition under in vivo conditions (Lou et al., 2020; Luo et al., 2021; Yang et al., 2021). However, our understanding of the in vitro succession of gut microbial communities is limited. Establishing stable microbial communities in bioreactors through in vitro succession of the worm gut microbiomes has important practical significance. In vitro incubation avoids the interference of worm physiological processes with the gut microbiomes, facilitating the establishment of potential plastic-degrading microbial communities. The establishment of stable microbial communities through in vitro incubation is more practical for engineering applications. As a proof-of-concept, our study demonstrated the feasibility of enriching plastic-degrading bacteria through in vitro incubation of gut microbial communities from plastic-munching worms. Considering the larger community shift magnitude and better practicality in the second-stage enrichment, the in vitro enrichment strategy is promising for applications in bioprocessing of plastic wastes. The established microbial communities on plastics are also potential microbial resources for the mining of plastic-degrading enzymes and bacterial strains.

In our analyses of enriched genera, we mainly focused on the differentially abundant genera which contain known plastic degraders. However, given the insufficient research on the functions of gut microbes in the worms (Pivato et al., 2022; Ru et al., 2020), many enriched bacteria may be potential plastic degraders that have not been previously reported. For example, differentially abundant genera, such as *Morganella* in the HDPE-associated biofilm communities and *Methylobacterium* in the PS-associated biofilm communities should be further assessed for their potential plastic-degrading capabilities. Moreover, the known degradation scopes of plastic degraders are also inadequate (Pivato et al., 2022). As conventional studies of plastic biodegradation only included limited types of plastics, the assessments of plastic-degradation capabilities were often incomplete. Given the similar chemical structures of commonly used plastics (Brandon et al., 2018; Ellis et al., 2021), the degradation capability of plastic-degrading bacteria should not be restricted to limited types of plastics. Our results revealed possible wider degradation scope for known degraders, for

instance, while *Ochrobactrum*, *Alcaligenes*, and *Acinetobacter* have not been reported capable of degrading PP, they were enriched in the PP-associated biofilm communities. Similarly, *Stenotrophomonas* has not been reported to be able to degrade PS but was enriched in the PS-associated biofilm communities. Our community succession analyses can only imply the establishment of potential plastic-degrading microbial communities through in vitro incubation of the gut microbiomes from plastic-munching worms. Further characterization of the enriched taxa in plastic-associated biofilm communities is needed in the future.

5. Conclusions

Using the gut microbiome of a plastic-munching worm, *Zophobas atratus*, we established plastic-associated biofilm communities through a two-stage enrichment process: change of the diet from oatmeal to plastics (HDPE, PP, and PS) and in vitro incubation of gut microbiomes with plastics. Plastic feeding exhibited a marginal influence on bacterial diversity but substantially changed the relative abundance of different bacterial groups, and intriguingly, enriched potential plastic degraders. More prominent shifts of microbial communities were observed during the in vitro incubation of the gut microbiomes with plastics. Taxa that contain reported plastic-degrading strains were further enriched during the in vitro incubation, and deterministic ecological effects were identified as the main driving force of the observed community shifts. Our findings improve our understanding of microbial community succession during the in vitro incubation of gut microbiomes from plastic-munching worms. Our strategy to establish plastic-associated microbial communities in bioreactors has important practical significance towards plastic-munching-worm-inspired bioprocessing of plastic wastes.

CRediT authorship contribution statement

Yi-Nan Liu: Writing – original draft, Investigation, Conceptualization. **Sakcham Bairoliya:** Writing – original draft, Investigation, Data curation. **Norazean Zaiden:** Methodology, Investigation. **Bin Cao:** Writing – review & editing, Supervision, Funding acquisition, Conceptualization.

Declaration of Competing Interest

The authors declare that they have no known competing financial interests or personal relationships that could have appeared to influence the work reported in this paper.

Data availability

The raw sequencing data have been deposited in the NCBI SRA database (BioProject ID: PRJNA948638). The R scripts used in the processing of the sequencing data are available in the GitHub repository (https://github.com/liuyinan19922/Worm-gut-microbiome).

Acknowledgments

This research was supported by the Accelerating Creativity and Excellence (ACE) grant (Award no.: NTU-ACE2021-01 to B.C.), Nanyang Technological University, Singapore, and by the NRF and Ministry of Education Singapore under its Research Centre of Excellence Programme, Singapore Centre for Environmental Life Sciences Engineering (M4330005.C70 to B.C.), Nanyang Technological University, Singapore.

Appendix A. Supplementary data

Supplementary data to this article can be found online at https://doi.org/10.1016/j.envint.2023.108349.

References

Amaral-Zettler, L.A., Zettler, E.R., Mincer, T.J., 2020. Ecology of the plastisphere. Nat. Rev. Microbiol. 18, 139–151.
Arunrattiyakorn, P., Ponprateep, S., Kaennonsang, N., Charapok, Y., Punphuet, Y., Krajangsang, S., Tangteerawatana, P., Limtrakul, A., 2022. Biodegradation of polystyrene by three bacterial strains isolated from the gut of Superworms (Zophobas atratus larvae). J. Appl. Microbiol. 132, 2823–2831.
Billen, P., Khalifa, L., Van Gerven, F., Tavernier, S., Spatari, S., 2020. Technological application potential of polyethylene and polystyrene biodegradation by macro-organisms such as mealworms and wax moth larvae. Sci. Total Environ. 735, 139521.
Brandon, A.M., Gao, S.-H., Tian, R., Ning, D., Yang, S.-S., Zhou, J., Wu, W.-M., Criddle, C. S., 2018. Biodegradation of polyethylene and plastic mixtures in mealworms (larvae of tenebrio molitor) and effects on the gut microbiome. Environ. Sci. Tech. 52, 6526–6533.
Callahan, B.J., McMurdie, P.J., Rosen, M.J., Han, A.W., Johnson, A.J.A., Holmes, S.P., 2016. DADA2: High-resolution sample inference from Illumina amplicon data. Nat. Meth. 13, 581–583.
Coates, J., 2006. Interpretation of Infrared Spectra. A Practical Approach, Encyclopedia of Analytical Chemistry.
Danso, D., Schmeisser, C., Chow, J., Zimmermann, W., Wei, R., Leggewie, C., Li, X., Hazen, T., Streit, W.R., 2018. New Insights into the Function and Global Distribution of Polyethylene Terephthalate (PET)-Degrading Bacteria and Enzymes in Marine and Terrestrial Metagenomes. Appl. Environ. Microbiol. 84, e02773–e12717.
Djemiel, C., Maron, P.-A., Terrat, S., Dequiedt, S., Cottin, A., Ranjard, L., 2022. Inferring microbiota functions from taxonomic genes: a review. GigaScience 11, giab090.
Douglas, G.M., Maffei, V.J., Zaneveld, J.R., Yurgel, S.N., Brown, J.R., Taylor, C.M., Huttenhower, C., Langille, M.G.I., 2020. PICRUSt2 for prediction of metagenome functions. Nat. Biotechnol. 38, 685–688.
Ellis, L.D., Rorrer, N.A., Sullivan, K.P., Otto, M., McGeehan, J.E., Román-Leshkov, Y., Wierckx, N., Beckham, G.T., 2021. Chemical and biological catalysis for plastics recycling and upcycling. Nat. Catal. 4, 539–556.
Galloway, T.S., Cole, M., Lewis, C., 2017. Interactions of microplastic debris throughout the marine ecosystem. Nat. Ecol. Evol. 1, 0116.
Gambarini, V., Pantos, O., Kingsbury, J.M., Weaver, L., Handley, K.M., Lear, G., 2022. PlasticDB: a database of microorganisms and proteins linked to plastic biodegradation. Database 2022.
Hajighasemi, M., Tchigvintsev, A., Nocek, B., Flick, R., Popovic, A., Hai, T., Khusnutdinova, A.N., Brown, G., Xu, X., Cui, H., Anstett, J., Chernikova, T.N., Brüls, T., Le Paslier, D., Yakimov, M.M., Joachimiak, A., Golyshina, O.V., Savchenko, A., Golyshin, P.N., Edwards, E.A., Yakunin, A.F., 2018. Screening and characterization of novel polyesterases from environmental metagenomes with high hydrolytic activity against synthetic polyesters. Environ. Sci. Tech. 52, 12388–12401.
Hatti-Kaul, R., Chen, L., Dishisha, T., Enshasy, H.E., 2018. Lactic acid bacteria: From starter cultures to producers of chemicals. FEMS Microbiol. Lett. 365, fny213.
Jambeck, J.R., Geyer, R., Wilcox, C., Siegler, T.R., Perryman, M., Andrady, A., Narayan, R., Law, K.L., 2015. Plastic waste inputs from land into the ocean. Science 347, 768–771.
Jiang, S., Su, T., Zhao, J., Wang, Z., 2021. Isolation, identification, and characterization of polystyrene-degrading bacteria from the gut of galleria mellonella (Lepidoptera: Pyralidae) larvae. Front. Bioeng. Biotechnol. 9, 736062.
Kembel, S.W., Cowan, P.D., Helmus, M.R., Cornwell, W.K., Morlon, H., Ackerly, D.D., Blomberg, S.P., Webb, C.O., 2010. Picante: R tools for integrating phylogenies and ecology. Bioinformatics 26, 1463–1464.
Kim, H.R., Lee, H.M., Yu, H.C., Jeon, E., Lee, S., Li, J., Kim, D.-H., 2020. Biodegradation of polystyrene by Pseudomonas sp. isolated from the gut of superworms (larvae of Zophobas atratus). Environ. Sci. Tech. 54, 6987–6996.
Leslie, H.A., van Velzen, M.J.M., Brandsma, S.H., Vethaak, A.D., Garcia-Vallejo, J.J., Lamoree, M.H., 2022. Discovery and quantification of plastic particle pollution in human blood. Environ. Int. 163, 107199.
Lou, Y., Ekaterina, P., Yang, S.-S., Lu, B., Liu, B., Ren, N., Corvini, P.F.X., Xing, D., 2020. Biodegradation of polyethylene and polystyrene by greater wax moth larvae (Galleria mellonella L.) and the effect of co-diet supplementation on the core gut microbiome. Environ. Sci. Tech. 54, 2821–2831.
Louca, S., Parfrey, L.W., Doebeli, M., 2016. Decoupling function and taxonomy in the global ocean microbiome. Science 353, 1272–1277.
Luo, L., Wang, Y., Guo, H., Yang, Y., Qi, N., Zhao, X., Gao, S., Zhou, A., 2021. Biodegradation of foam plastics by Zophobas atratus larvae (Coleoptera: Tenebrionidae) associated with changes of gut digestive enzymes activities and microbiome. Chemosphere 282, 131006.
McMurdie, P.J., Holmes, S., 2013. phyloseq: an R package for reproducible interactive analysis and graphics of microbiome census data. PLoS One 8, e61217.
Ning, D., Yuan, M., Wu, L., Zhang, Y., Guo, X., Zhou, X., Yang, Y., Arkin, A.P., Firestone, M.K., Zhou, J., 2020. A quantitative framework reveals ecological drivers of grassland microbial community assembly in response to warming. Nat. Commun. 11, 4717.
Nizzetto, L., Langaas, S., Futter, M., 2016. Pollution: do microplastics spill on to farm soils? Nature 537, 488.
Oksanen, J., Blanchet, F.G., Friendly, M., Kindt, R., Legendre, P., McGlinn, D., Minchin, P., O'Hara, R., Simpson, G., Solymos, P., 2020. vegan: Community Ecology Package. R Package Version 2 (5–7), 2022.
Parks, D.H., Tyson, G.W., Hugenholtz, P., Beiko, R.G., 2014. STAMP: statistical analysis of taxonomic and functional profiles. Bioinformatics 30, 3123–3124.

Peng, B.-Y., Su, Y., Chen, Z., Chen, J., Zhou, X., Benbow, M.E., Criddle, C.S., Wu, W.-M., Zhang, Y., 2019. Biodegradation of polystyrene by dark (tenebrio obscurus) and yellow (tenebrio molitor) mealworms (coleoptera: tenebrionidae). Environ. Sci. Tech. 53, 5256–5265.
Pessione, E., 2012. Lactic acid bacteria contribution to gut microbiota complexity: lights and shadows. Front. Cell. Infect. Microbiol. 2, 86.
Pivato, A.F., Miranda, G.M., Prichula, J., Lima, J.E., Ligabue, R.A., Seixas, A., Trentin, D. S., 2022. Hydrocarbon-based plastics: Progress and perspectives on consumption and biodegradation by insect larvae. Chemosphere 133600.
Ragaert, K., Delva, L., Van Geem, K., 2017. Mechanical and chemical recycling of solid plastic waste. Waste Manag. 69, 24–58.
Roser, H.R.a.M. Plastic Pollution. Published online at OurWorldInDataorg; 2022.
Ru, J., Huo, Y., Yang, Y., 2020. Microbial degradation and valorization of plastic wastes. Front. Microbiol. 11, 442.
Sanluis-Verdes, A., Colomer-Vidal, P., Rodriguez-Ventura, F., Bello-Villarino, M., Spinola-Amilibia, M., Ruiz-Lopez, E., Illanes-Vicioso, R., Castroviejo, P., Aiese Cigliano, R., Montoya, M., Falabella, P., Pesquera, C., Gonzalez-Legarreta, L., Arias-Palomo, E., Solà, M., Torroba, T., Arias, C.F., Bertocchini, F., 2022. Wax worm saliva and the enzymes therein are the key to polyethylene degradation by Galleria mellonella. Nat. Commun. 13, 5568.
Schwabl, P., Köppel, S., Königshofer, P., Bucsics, T., Trauner, M., Reiberger, T., Liebmann, B., 2019. Detection of various microplastics in human stool: a prospective case series. Ann. Intern. Med. 171, 453–457.
Wei, R., Tiso, T., Bertling, J., O'Connor, K., Blank, L.M., Bornscheuer, U.T., 2020. Possibilities and limitations of biotechnological plastic degradation and recycling. Nat. Catal. 3, 867–871.
Wright, R.J., Bosch, R., Gibson, M.I., Christie-Oleza, J.A., 2020. Plasticizer degradation by marine bacterial isolates: a proteogenomic and metabolomic characterization. Environ. Sci. Tech. 54, 2244–2256.
Yang, K., Chen, Q.-L., Chen, M.-L., Li, H.-Z., Liao, H., Pu, Q., Zhu, Y.-G., Cui, L., 2020. Temporal dynamics of antibiotic resistome in the plastisphere during microbial colonization. Environ. Sci. Tech. 54, 11322–11332.
Yang, S.-S., Ding, M.-Q., He, L., Zhang, C.-H., Li, Q.-X., Xing, D.-F., Cao, G.-L., Zhao, L., Ding, J., Ren, N.-Q., Wu, W.-M., 2021. Biodegradation of polypropylene by yellow mealworms (Tenebrio molitor) and superworms (Zophobas atratus) via gut-microbe-dependent depolymerization. Sci. Total Environ. 756, 144087.
Yang, J., Yang, Y., Wu, W.M., Zhao, J., Jiang, L., 2014. Evidence of polyethylene biodegradation by bacterial strains from the guts of plastic-eating waxworms. Environ. Sci. Tech. 48, 13776–13784.
Yeom, S.-J., Le, T.-K., Yun, C.-H., 2022. P450-driven plastic-degrading synthetic bacteria. Trends Biotechnol. 40, 166–179.
Yoshida, S., Hiraga, K., Takehana, T., Taniguchi, I., Yamaji, H., Maeda, Y., Toyohara, K., Miyamoto, K., Kimura, Y., Oda, K., 2016. A bacterium that degrades and assimilates poly(ethylene terephthalate). Science 351, 1196–1199.
Zhang, Y., Pedersen, J.N., Eser, B.E., Guo, Z., 2022b. Biodegradation of polyethylene and polystyrene: From microbial deterioration to enzyme discovery. Biotechnol. Adv. 60, 107991.
Zhang, Z., Peng, H., Yang, D., Zhang, G., Zhang, J., Ju, F., 2022c. Polyvinyl chloride degradation by a bacterium isolated from the gut of insect larvae. Nat. Commun. 13, 5360.
Zhang, F., Wang, F., Wei, X., Yang, Y., Xu, S., Deng, D., Wang, Y.-Z., 2022a. From trash to treasure: Chemical recycling and upcycling of commodity plastic waste to fuels, high-valued chemicals and advanced materials. J Energy Chem 69, 369–388.